Analyst

ROYAL SOCIETY OF CHEMISTRY

PAPER

View Article Online
View Journal | View Issue

Cite this: *Analyst*, 2025, **150**, 4630

Comparison of solid phase microextraction geometries for effective preconcentration of volatile per- and polyfluoroalkyl substances

Madison L. Williams,[a] Stefan Cretnik,[b] Lucas Lüthy,[b] Tom Flug,[b] Michael Stebler[b] and Emanuela Gionfriddo *[a]

Neutral per- and polyfluoroalkyl substances (PFAS) serve as precursors to perfluorinated acids, and their transformation contributes to the ongoing release of legacy PFAS contaminants into the environment. The accurate and efficient extraction of neutral, volatile PFAS remains a critical analytical challenge. In this study, we evaluated the impact of solid phase microextraction (SPME) geometry and agitation methods on extraction performance using SPME-fiber and SPME-arrow devices in headspace (HS) and direct immersion (DI) extraction modes. Agitation of the samples during extraction was conducted with a cycloid-shaped Heatex agitator at 600 rpm and compared to an orbital shaker at 250 rpm. Results demonstrated that SPME-arrow devices offered enhanced sensitivity and broader linear dynamic ranges for fluorotelomer alcohols such as 1*H*,1*H*,2*H*,2*H*-perfluoro-1-hexanol (4:2 FTOH). In contrast, SPME-fibers showed improved response for hydrophobic, semi-volatile analytes such as *N*-methylperfluorooctanesulfonamidoethanol (MeFOSE) with lower limits of quantitation (0.005 μg L^{-1}–0.25 μg L^{-1}). The influence of extraction mode on SPME-geometry was systematically investigated with residual plots (DI-HS) reaffirming the propensity for extraction by DI of hydrophobic, semi-volatile analytes and volatile analytes by HS. The Heatex agitator improved extraction efficiency for diffusion-limited compounds by enhancing convective mixing and reducing mass transfer resistance in the boundary layer. Extraction time profiles suggested the occurrence of competitive adsorption at extraction times longer than 35 min. These findings underscore the importance of tailoring SPME parameters – agitation type, extraction mode, time, and sorbent geometry – when developing sample preparation workflows for analysis of neutral volatile PFAS.

Received 19th July 2025,
Accepted 6th September 2025

DOI: 10.1039/d5an00758e

rsc.li/analyst

1 Introduction

Per- and polyfluoroalkyl substances (PFAS) are a class of synthetic organic chemicals that contain a carbon backbone fully or partially substituted by fluorine atoms. Their unique physicochemical properties, including hydrophobicity, oleophobicity, and exceptional chemical and thermal stability, have led to widespread use in industrial and consumer products.[1] However, these same properties contribute to their environmental persistence, potential for bioaccumulation, and resistance to degradation.[2–4] Exposure to certain PFAS has been linked to adverse health outcomes such as immunotoxicity, reproductive toxicity, and carcinogenicity.[2,4] As the toxicological effects of PFAS become better understood, they have spurred increased scientific interest in the development of characterization and remediation techniques. Among the most extensively studied PFAS are long-chain perfluoroalkane sulfonates and perfluorocarboxylates (C4–C15), namely perfluorooctanoic acid (PFOA) and perfluorooctane sulfonate (PFOS). Due to their non-volatile and lower water solubility, exposure sources for these substances can be attributed to either direct transfer, such as dietary intake, or indirect transfer through the metabolic transformation of perfluoroalkyl acids (PFAA) precursors.[5] Neutral, volatile PFAA precursors can be converted into more persistent and toxic PFAS with longer biological half-lives, contributing to the overall presence of ionic PFAS within environmental systems.[3]

Large-scale PFAS synthesis commonly involves telomerization, a process in which smaller fluorocarbon building blocks condense to produce perfluoroalkyl iodides with a range of carbon atoms. These intermediates can subsequently undergo further reactions to generate fluorotelomer alcohols (FTOHs) and fluorotelomer olefins (FTOs), which may be emitted into

[a]*Department of Chemistry, University at Buffalo, The State University of New York, Buffalo, New York 14260-3000, USA. E-mail: egionfri@buffalo.edu*
[b]*CTC Analytics AG, Industriestrasse 20, 4222 Zwingen, Switzerland*

the environment during the manufacturing process or as industrial waste.[6,7] Compared to their non-fluorinated analogs, the presence of weak van der Waals interactions leads to higher vapor pressure, resulting in increased volatility of FTOHs and FTOs.[8] For example, the Henry's law constant (K_H) of 1-hexanol is approximately 1.71×10^{-3} atm m^3 mol^{-1} while its fluorinated analog 4:2 FTOH, has a K_H of 7.6×10^{-3} atm m^3 mol^{-1}.[8–10] Given their central role in the manufacturing industry, the detection and quantification of volatile PFAA precursors is critical in understanding sources of PFAS within the environment and to enable an accurate mass balance for PFAS transformation processes. PFAS are predominantly analyzed *via* liquid chromatography coupled with tandem mass spectrometry (LC-MS/MS), using electrospray ionization (ESI).[11,12] However, LC-MS/MS methods face notable limitations in the simultaneous detection of ionic and non-ionic PFAS due to: (1) ionization suppression of FTOHs caused by buffered mobile phases, (2) limited ionizability of certain PFAA precursors under atmospheric pressure ionization, particularly those with high fluorine-to-carbon (F : C) ratios, and (3) the volatility of certain analytes, which can hinder their retention and quantification.[5,7,13] As a result, gas chromatography coupled with mass spectrometry (GC-MS) has emerged as a valuable tool for analyzing neutral volatile PFAS. Due to the ultra-trace concentrations at which these compounds are present in environmental samples, they present significant analytical challenges, including achieving effective preconcentration prior to GC-MS.[6,14] To address these limitations, the incorporation of targeted extraction techniques that can enhance analyte preconcentration and improve method sensitivity is needed.[15]

To this end, techniques such as dynamic headspace extraction (DHS), capture *via* thermal desorption (TD) tubes, and solid phase extraction (SPE), are increasingly used for the determination of volatile PFAS in environmental samples.[16–18] Considered the gold standard for analysis of ionizable PFAS, SPE can suffer from insufficient extract cleanup, breakthrough, and low recoveries due to the loss of volatile compounds during handling. While successfully applied for sampling of volatile PFAS, TD has also been associated with the potential thermal degradation of PFOA to perfluoro-1-heptene upon desorption, leading to the detection of the degradation product rather than the native compound.[14,19] Notably, the combination of DHS and TD, achieved limits of quantification for FTOHs down to low parts-per-trillion levels (6.57 ng L^{-1}) when used in tandem with zers time-of-flight mass spectrometers.[16] While each sample preparation approach offers distinct advantages; they also have associated limitations and can require multiple steps. Solid phase microextraction (SPME) is a complementary alternative that integrates sampling, extraction, and preconcentration into a single solvent-free step. Requiring minimal sample preparation, SPME is easily automated and can reduce potential analyte loss, making it an attractive alternative for high-throughput workflows.[20] The portability of SPME enables rapid on-site sampling, making it suitable for applications where sample transportation is cumbersome or when continuous sampling is required.[21,22] SPME-fibers with an extraction phase of Divinylbenzene/Carboxen/Polydimethylsiloxane (DVB/Car/PDMS) have been successfully used for the extraction of volatile PFAA precursors from both aqueous and gaseous samples at ultra-trace levels of 5 ng L^{-1} and <5 ng L^{-1}, respectively.[15] Even so, the key limitation of commercially available SPME-fibers lies in their relatively small sorbent phase volume (0.028–0.612 μL), which can restrict analyte loading capacity and ultimately limit sensitivity.[20]

SPME-arrows represent an alternative extraction geometry that retain the advantages of commercial SPME-fibers, while excluding their drawbacks. Featuring a significantly larger extraction phase volume (3.8–11.8 μL) immobilized on a stainless-steel rod, SPME-arrows have been shown to increase extraction capacity and reproducibility.[23,24] This higher sorbent surface-to-volume ratio in SPME-arrows compared to SPME-fibers can enhance extraction kinetics, a critical advantage for quantifying volatile PFAS at ultra-trace levels.[24] Additionally, extraction phases used for commercial SPME-fibers are also available in SPME-arrow format. Given that DVB/Car/PDMS SPME-fibers have demonstrated successful extraction of volatile PFAS at low concentrations, it follows that SPME-arrows employing the same sorbent chemistry should exhibit comparable, if not superior, performance. In this work, two different SPME extraction geometries, arrow and fiber, were systematically assessed for their ability to preconcentrate and extract 6 volatile PFAS. Headspace (HS) and direct immersion (DI) extraction modes were investigated to assess performance under varying sample conditions. The effect of agitation method on extraction efficiency was explored by comparing the cycloid-shaped mixing motion of the Heatex to the orbital shaker (OS). Results demonstrated that the combination of HS-SPME-arrow with Heatex agitation yielded lower limits of detection (LODs) and quantification (LOQs), as well as broader linear dynamic ranges relative to other tested configurations.

2 Experimental conditions and methods

2.1 Reagents and materials

Individual standard solutions of PFAS in methanol (50 or 100 mg L^{-1}), namely 1*H*,1*H*,2*H*,2*H*-perfluoro-1-hexanol (4:2 FTOH), 1*H*,1*H*,2*H*,2*H*-perfluoro-1-octanol (6:2 FTOH), 1*H*,1*H*,2*H*,2*H*-perfluoro-1-decanol (8:2 FTOH), *N*-ethyl Perfluorooctanesulfonamide (EtFOSA), and *N*-methylperfluoro octanesulfonamidoethanol (MeFOSE) were purchased from AccuStandard® Inc. (Connecticut, USA); and *N*,*N*-dimethyl-*n*-perfluorooctanesulfonamide (Me_2FOSA) from Wellington Laboratories (Ontario, Canada). Internal standards, including *N*-ethyl-d_5-perfluoro-1-octanesulfonamide and 1,2-$^{13}C_2$,1,1,2,2-D_4 8:2 fluorotelomer alcohol (D_5-EtFOSA and 1,2-C_{13},1,1,2,2-D_4-8:2 FTOH), were purchased from Cambridge Isotope Laboratories, Inc. (Massachusetts, USA). Per manufacturer's instructions, PFAS standards were stored at −20 °C or room

temperature. Details regarding the organofluorine compounds can be found in the SI in Table S1. Working standard solutions were prepared daily by diluting stock solutions in methanol. Ultrapure water (UPW) (18.2 MΩ cm) was sourced from an Alto™-i Type 1 Ultrapure Water Purification System by Avidity Science (Wisconsin, USA).

Commercial 10 mm SPME-fibers were provided by CTC Analytics (Zwingen, Switzerland), in an automated format with an 80 μm thick extraction phase consisting of Divinylbenzene/Carbon Wide Range/Polydimethylsiloxane (DVB/C-WR/PDMS). Similarly, commercial 1.10 mm SPME-arrows with a 120 μm thick extraction phase of DVB/C-WR/PDMS were provided by CTC Analytics (Zwingen, Switzerland), and assessed. Prior to use and periodically within experimental sets, SPME fibers and arrows were conditioned according to the manufacturer's guidelines.

2.2 Instrumentation

Chromatographic separation and detection were performed using an Agilent 8890/5997C gas chromatograph-mass spectrometer (GC-MS) system equipped with a split/splitless inlet and ultra-high purity helium gas (99.999%), sourced from AirGas (Pennsylvania, USA), was used as the carrier gas. Injections were performed using a Multipurpose Sampler (MPS) autosampler, equipped for automated SPME (Gerstel, Inc., Maryland, USA) using a CTC SPME arrow liner (ID 1.7 mm, for split/splitless injector). An Agilent HP-5MS UI capillary column (30 m, 0.25 mm i.d., 0.25 μm film thickness) was used to achieve chromatographic separation. A constant flow rate of 1.0 mL min^{-1} was maintained during the temperature program which started at 50 °C for 2 min, followed by a ramp of 15 °C per min to 120 °C, held for 1 min, before increasing to 300 °C at a rate of 40 °C min^{-1} and held for 1 min, resulting in a total run time of 13.2 min. Mass spectrometry was accomplished using electron ionization (EI) at 70 eV, with the following conditions: ion source temperature, 230 °C; quadrupole temperature, 150 °C; and transfer line temperature, 280 °C. Data were aquired in single ion monitoring (SIM) mode; ions monitored for quantification are provided in bold in Table S1.

Data acquisition and processing were performed using MassHunter Workstation: quantitative analysis (version 12.0, Build 12.0.893.1) (Agilent Technologies, California, USA). Origin 9.0 (OriginLab Corporation, Massachusetts, USA) was used for additional data processing. Scanning electron microscopy (SEM) (Carl Zeiss AURIGA, CrossBeam, California, USA) was employed to characterize the surface and cross-section of the SPME-arrow.

2.3 SPME methodology

For DI optimization experiments, 10 mL clear round-bottom vials (Verex Headspace Vial, 23 × 46 mm, 18 mm screw cap, Phenomenex, California, USA) were filled with 9 mL of aqueous PFAS mixture, and incubation times of 2 min, 5 min, and 10 min were evaluated. For HS optimization, 20 mL clear round-bottom vials (Verex Headspace Vial, 23 × 75 mm, 18 mm screw cap, Phenomenex, California, USA) containing 9 mL of the same aqueous PFAS mixture were used, and incubation times of 5 min, 15 min, and 25 min were assessed. In all experiments, samples were freshly prepared and analyzed immediately to minimize analyte loss. Based on previous work from our group, extraction temperatures were set to 60 °C for direct immersion (DI) and 50 °C for headspace (HS) conditions, followed by a 5 min desorption at 270 °C in splitless mode. Once the desorption was completed, the purge valve was opened for 5 min at a flow rate of 100 mL min^{-1}, and the gas saver mode was activated at 5.1 min. Optimization was conducted based on extraction mode rather than sorbent geometry, with parameters tailored accordingly. For both extraction modes, extraction times ranging from 5 to 90 min were evaluated using an orbital shaker (OS) at 250 rpm and a Heatex agitator at 600 rpm, to identify the optimal conditions for analyte extraction efficiency. The OS was operated at its default extraction speed of 250 rpm, which is recommended to prevent potential damage to the SPME fiber. All experiments were performed in triplicate using independent samples; subsequent fiber blanks did not reveal carryover of the analytes.

Method validation was conducted in HS mode under optimized conditions—samples were incubated at 50 °C and agitated at 600 rpm for 25 min, followed by a 20 min extraction and a 5 min desorption. A series of aqueous standards at concentrations of 0.005, 0.05, 0.1, 0.25, 0.5, 1, 2.5, 5, 10, and 25 μg L^{-1} were prepared to assess the impact of extraction geometry on the linear dynamic range for HS-SPME. Each concentration level was tested in triplicate using independently prepared samples to ensure reproducibility and statistical reliability. Internal standards, including *N*-ethyl-d_5-perfluoro-1-octanesulfonamide and 1,2-$^{13}C_2$,1,1,2,2-D_4 8:2 fluorotelomer alcohol (D_5-EtFOSA and 1,2-C_{13},1,1,2,2-D_4-8:2 FTOH) were added to each sample at a final individual concentration of 5 μg L^{-1}. Method performance was evaluated by determining linearity, accuracy, precision, limit of detection (LOD), limit of quantitation (LOQ), and the linear dynamic range for both SPME geometries. Linearity was further assessed using lack-of-fit test.[25]

3 Results and discussion

3.1 Optimization of SPME geometry and extraction mode

Headspace extraction *via* SPME is limited by the mass transfer of analytes from the bulk sample to the headspace, which is correlated to the analyte's Henry's Law constant. Moreover, the kinetics of the mass transfer between the liquid and gaseous phase are based on Fick's laws of diffusion.[26–28] In the case of DI, the rate of extraction is correlated to the diffusion of analytes through the extraction phase and across the diffusion boundary layer surrounding the extraction phase.[29–31] As the extraction phase volume of the SPME device increases, so too does analytical sensitivity and extraction efficiency, as in the instance of SPME-fiber to SPME-arrow.[27] To investigate the combined effects of geometry and extraction mode, residual response plots (DI–HS) were generated over an extraction time range (5 to 90 min) using a Heatex agitator at 600 rpm for the

SPME-fiber (Fig. 1A) and SPME-arrow (Fig. 1B) as analytes approached equilibrium under HS and DI conditions. Positive values indicate greater response in DI mode, while negative values reflect higher response in HS mode. Among the FTOHs, 4:2 FTOH exhibited consistently negative residuals for both geometries across all time points, indicating greater extraction efficiency in HS, regardless of extraction time. This trend reflects 4:2 FTOHs Henry's law constant (7.6×10^{-3} atm m^3 mol^{-1}), which facilitates rapid and efficient volatilization into the headspace, making it highly amenable to HS-SPME regardless of SPME geometry.[9] At shorter extraction times for the SPME-arrow, residual values for 6:2 FTOH were near zero, indicating comparable extraction efficiency between DI and HS modes. However, as extraction time increased, residuals became strictly positive, suggesting enhanced extraction by DI with extended extraction times. For the SPME-fiber, the residual plot for 6:2 FTOH exhibited a negative value at the earliest time point (5 min), shifting progressively toward positive values with increasing extraction time. In contrast, 8:2 FTOH exhibited the opposite trend: extraction with the SPME-arrow favored DI, while extraction with the SPME-fiber showed greater efficiency in HS mode. Regardless of SPME geometry, the semi-volatile and more hydrophobic analytes—Me_2FOSA, EtFOSA, and MeFOSE, were consistently extracted with greater efficiency by DI compared to HS, with this trend becoming more pronounced as the extraction time increased. This behavior can be attributed to their decreased volatility when compared to the FTOHs, which can limit their partitioning into the HS. While the impact of ionic strength on SPME extraction efficiency was not examined in the present study, its importance as a parameter for optimization cannot be overlooked. Previous work from our group has investigated the role of ionic strength for a similar suite of volatile PFAS.[15]

3.2 Comparative analysis of commercial agitation devices

There are several approaches to accelerate HS-SPME kinetics. The simplest of these include increasing temperature, which

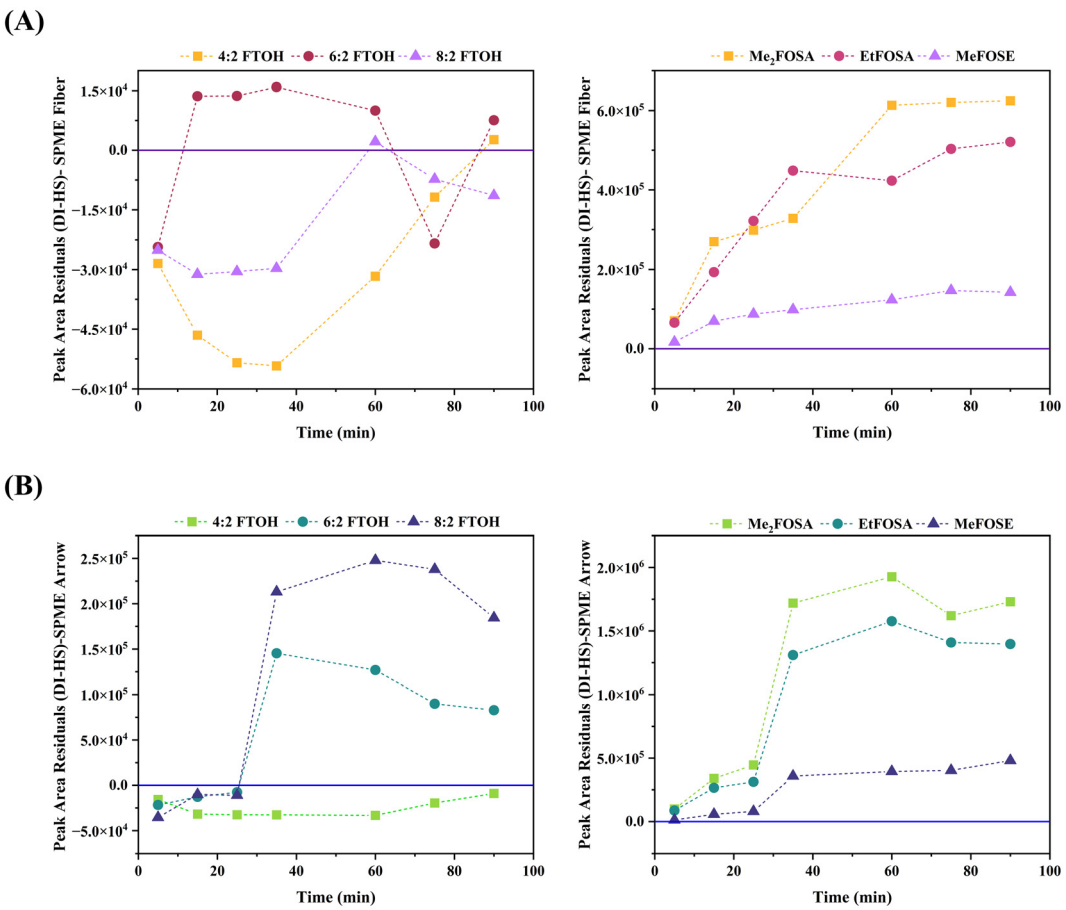

Fig. 1 Residual plot analysis comparing the difference in analyte response over time between HS and DI for (A) fiber and (B) arrow. Differences between analyte responses at different time points using DI and HS are plotted. When the value is above 0, it is indicative that the DI response is higher than HS at those time points, while when the value is below 0, it indicates that the HS response is greater than DI. Conditions for HS extractions were as follows: incubation (20 min) and extraction occurred at 50 °C, followed by a 5 min desorption. Analyte concentration was 0.5 μg L^{-1} 6:2 FTOH, 8:2 FTOH, Me_2FOSA, 1 μg L^{-1} EtFOSA, 2 μg L^{-1} 4:2 FTOH and 4 μg L^{-1} MeFOSE. Conditions for DI extractions were as follows: incubation (2 min) and extraction occurred at 60 °C, followed by a 5 min desorption. Analyte concentration was 2 μg L^{-1} 4:2 FTOH, 1 μg L^{-1} 6:2 FTOH, 8:2 FTOH, Me_2FOSA, EtFOSA, and 2 μg L^{-1} MeFOSE.

causes an increase in the analyte diffusion coefficient in the sample, and applying agitation, which reduces liquid–gas mass transfer resistance and minimizes the diffusion layer around the extraction device, causing a reduction in the concentration gradient in the boundary layer, allowing equilibrium to be attained faster.[28] Previous work has been conducted investigating the impact of temperature on the suite of PFAS in this study.[15] Since the FTOHs reach a maximum extraction efficiency at 50 °C, this temperature was selected for further HS-SPME experiments. In this work we evaluated the role of agitation, the application of an increased stirring rate, and a more efficient stirring mechanism, which can lead to a higher mass transfer rate of the analyte into the extraction phase.[32,33] The impact of agitation mechanism on the extraction kinetics was investigated for both SPME-fiber (Fig. S1) and arrow geometries (Fig. S2). While both the orbital shaker (OS) and Heatex introduce a mechanical motion to the liquid and gas phases within the vial, they differ in the pattern of shaking. Additionally, the default extraction speed of 250 rpm was used for the OS to avoid SPME-fiber damage, a concern not observed with the Heatex even at higher rpm. The Heatex promotes uniform heat distribution and improved thermal equilibration due to its cycloid-shaped mixing motion, thereby facilitating the headspace partitioning of more semi-volatile compounds.[33] This is reinforced by comparing the responses of the semi-volatile, later-eluting compounds, Me_2FOSA, EtFOSA, and MeFOSE, with both SPME-fiber and arrow. As the volatility of the analyte decreases, the benefit of Heatex agitation becomes more pronounced. For example, the use of the OS resulted in increased extraction efficiency of Me_2FOSA regardless of SPME geometry. Specifically, there was an average increase in extraction efficiency of 58% at the 75 min time point for OS when compared to Heatex for SPME-arrow. For EtFOSA, the OS achieved a 5% increase in extraction efficiency at the same time point when compared to the Heatex. Notably, for the least volatile analyte MeFOSE, the OS demonstrated a decrease of 68% compared to the Heatex agitator. A reduction in agitation speed can result in longer times to achieve equilibrium and can lead to reduced extraction in pre-equilibrium extraction conditions.[32,33] Therefore, when comparing the extraction response of 4:2 FTOH with SPME-arrow (Fig. S2), the positive impact of the increased rpm of the Heatex on extraction efficiency is expected. At 15 min, using the Heatex agitator at 600 rpm, the SPME-arrow had a 250% increase in extraction efficiency for 4:2 FTOH (peak area = 3.5×10^4) compared to the same time using the OS at 250 rpm (peak area = 1.0×10^4). A comparable, though less pronounced increase, was also observed for 4:2 FTOH when the SPME-fiber geometry was used at 15 min. The response with the Heatex agitator had 49% increased efficiency (peak area = 5.2×10^4) compared to the OS (peak area = 3.5×10^4) at the same time point (Fig. S1). While FTOHs and FOSE/FOSAs exhibited different behaviors depending on the agitator type, they followed similar trends across both extraction phase geometries. Greater variability was observed when the Heatex and SPME-arrow were used in combination, while the relative standard

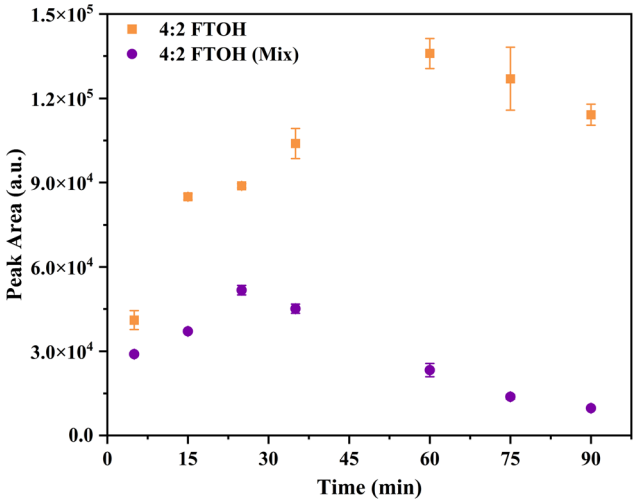

Fig. 2 Extraction time profiles of 4:2 FTOH extracted as part of a PFAS aqueous mixture (circle) and as an individual component (square). Extraction was conducted using an SPME-fiber in HS using an orbital shaker (OS); a temperature of 50 °C and 250 rpm was used for both incubation (25 min) and extraction, followed by a 5 min desorption. Analyte concentration was 2 μg L^{-1}.

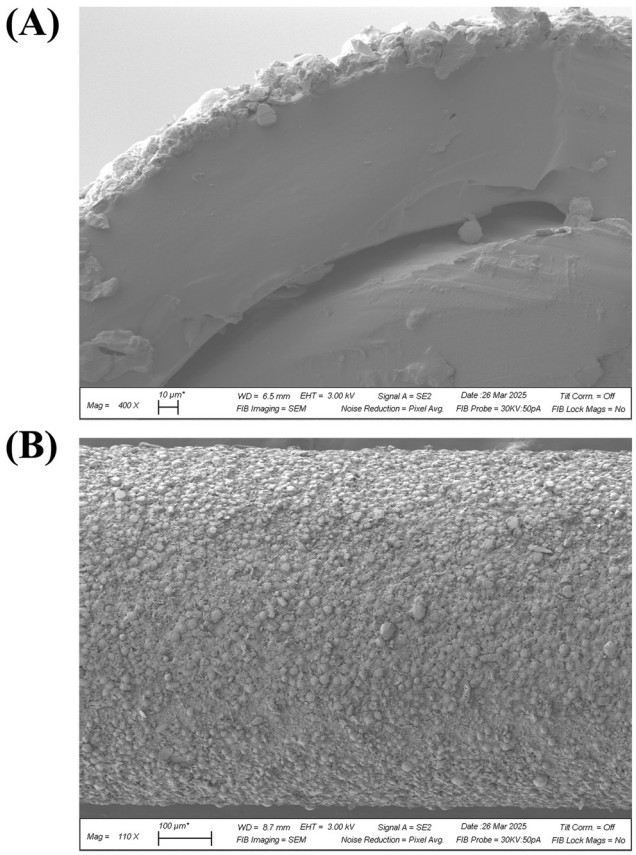

Fig. 3 Scanning electron microscopy (SEM) images showing a cross-section of the DVB/Car-WR/PDMS arrow (A) and a overview of the outer surface of the SPME-arrow (B).

deviation (RSD%) range for the OS agitator averaged between 0.6–10%, the Heatex agitator yielded RSD% values between 0.9–17%. This may be attributed to microleaks in the septa caused by the combination of high rpm and the larger diameter of the SPME-arrow device. This issue could be mitigated by testing alternative septa caps and employing analytical replicates. As the OS is manufacturer-limited to a maximum agitation speed of 250 rpm, it was not possible to determine whether the same phenomenon would occur with the OS at higher rpm.

3.3 Occurrence of competitive adsorption

When comparing the response of the most hydrophilic and volatile compounds (4:2 FTOH and 6:2 FTOH), analyte response decreased over extraction time. This effect was more pronounced with the SPME-fiber than the SPME-arrow, likely due to the fiber's smaller sorbent capacity and available adsorption sites. To probe the time-dependent decrease, the response of 4:2 FTOH was monitored as a single standard and within a multicomponent mixture (Fig. 2). When extracted *via* HS using the SPME-fiber in a mixture, the signal for 4:2 FTOH, the relatively most polar and volatile analyte, declined over time. However, this decrease did not occur when the extraction was repeated with 4:2 FTOH as a single component. These trends suggest that 4:2 FTOH is displaced from the DVB/Car-WR/PDMS extraction phase when extracted from a multicomponent mixture. At the time that 4:2 FTOH decreases in response, 35 min, the extraction efficiency of more hydrophobic analytes increases. This phenomenon may be attributed to competitive adsorption, whereby low-affinity compounds, such as 4:2 FTOH, are progressively replaced on the extraction phase by higher-affinity analytes, such as MeFOSE or EtFOSA, at longer extraction times.[34] This effect results in a measurable decrease in the response of the displaced analyte (4:2 FTOH) and a corresponding increase in the response of the displacing compounds (*i.e.*, MeFOSE and EtFOSA). The classical DVB/Car/PDMS extraction phase utilizes a multi-layer adsorbent system, whereby larger analytes first interact with the weaker DVB adsorbent while smaller analytes migrate deeper into the Car-PDMS layer for dual retention.[20,29] When DVB and Carboxen adsorbents are co-dispersed in PDMS at ratios equivalent to their respective single sorbent coatings, analytes migrate to the stronger adsorbent. SEM cross-sectional and surface imaging revealed a mixed-phase rather than multilayer morphology of the SPME-arrow coating (Fig. 3). This structural configuration likely promotes competitive adsorption phenomena, thereby amplifying displacement effects under prolonged extraction conditions.

3.4 Method validation

The method was validated for both SPME-fiber and arrow geometries in HS using the Heatex agitator at 600 rpm. Two isotopically labeled internal standards were also added from the FTOH and FOSA families. The concentration range covered

Table 1 Figures of merit for the HS-SPME-fiber GC-MS protocol

	LOD		LOQ			Precision (RSD, %)		Accuracy (%)	
Analytes	μg L^{-1}	*S*/*N*	μg L^{-1}	*S*/*N*	Accuracy (%) at LOQ	Intra-day[a]	Inter-day[b]	0.3 μg L^{-1}	3 μg L^{-1}
4:2 FTOH	0.005	11	0.05	32	113	5	9	121	120
6:2 FTOH	0.005	80	0.05	226	94	1	11	98	105
8:2 FTOH[c]	<0.005	—	1	4117	92	3	10	—	111
			0.005	98	102	4	10	103	—
Me_2FOSA	<0.005	—	0.005	242	111	4	3	97	103
EtFOSA	<0.005	—	0.005	345	91	2	7	94	104
MeFOSE	0.1	79	0.25	526	108	7	12	119	92

Dash (—) = concentration level not within linear dynamic range or determinable. [a] $n = 3$. [b] $n = 5$. [c] Multiple entries are related to distinct linear dynamic ranges, as reported in the SI (Table S2).

Table 2 Figures of merit for the HS-SPME-arrow GC-MS protocol

	LOD		LOQ			Precision (RSD, %)		Accuracy (%)	
Analytes	μg L^{-1}	*S*/*N*	μg L^{-1}	*S*/*N*	Accuracy (%) at LOQ	Intra-day[a]	Inter-day[b]	0.3 μg L^{-1}	3 μg L^{-1}
4:2 FTOH	<0.005	—	0.005	110	90	9	13	106	112
6:2 FTOH	0.005	40	0.05	756	111	5	8	98	109
8:2 FTOH	0.005	168	0.05	557	103	5	11	104	99
Me_2FOSA	<0.005	—	0.005	179	89	4	11	112	118
EtFOSA	<0.005	—	0.005	581	99	5	7	114	102
MeFOSE	0.1	450	0.5	603	91	8	9	—	117

Dash (—) = concentration level not within linear dynamic range or determinable. [a] $n = 3$. [b] $n = 5$.

was between 0.005 μg L^{-1} and 25 μg L^{-1}. Results pertaining to the linear dynamic range, regression equation, and coefficient can be found in Table S2 for SPME-fiber and S3 for SPME-arrow. The most hydrophobic analyte MeFOSE, had a lower LOQ (0.25 μg L^{-1}) and LOD (0.1 μg L^{-1}) with the SPME-fiber (Fig. S3 and S4). For the most volatile analytes, 4:2 FTOH and 6:2 FTOH, the SPME-arrow demonstrated greater linearity and sensitivity compared to fiber geometry with LODs as low as 0.005 μg L^{-1} (Fig. S5 and S6). SPME-arrow also demonstrated a single broad linear dynamic range for all analytes, compared to SPME-fiber. Regression coefficients, ranging from 0.9774 to 0.9955 for SPME-fiber and 0.9734 to 0.9984 for SPME-arrow, as well as lack-of-fit testing, confirmed the method's linearity within the reported ranges (p-value > 0.05). Furthermore, both fiber and arrow geometries demonstrated good precision, with RSD values ranging from 1–12% for SPME-fiber and 4–13% for SPME-arrow. Finally, accuracy was assessed by spiking ultrapure water at two different levels, 3 μg L^{-1} and 0.3 μg L^{-1}. Under these conditions, recoveries between 94 and 119% were obtained (Tables 1 and 2).

4 Conclusion

The results obtained in our work demonstrate the impact alternative agitation methods and extraction phase geometries have on the preconcentration of volatile PFAS. Here, we provide a thorough investigation into how increasing extraction phase thickness, agitation speed, and agitation mode can impact linear dynamic range, sensitivity, and extraction efficiency. SPME-arrows generally provided broader linear dynamic ranges (0.005 μg L^{-1}–25 μg L^{-1}) and higher regression coefficients (R^2 > 0.99), apart for Me_2FOSA, when compared to SPME-fibers. This is especially true for FTOHs, such as 4:2 and 6:2 FTOH. A comparison of cycloid-shaped mixing (Heatex) to orbital shaking (OS) showed that for the most hydrophobic analytes, such as MeFOSE, multidirectional motion increases their transfer to the HS and, therefore, their adsorption by the extraction phase. The extraction time profiles for the most polar and volatile analytes (*i.e.*, 4:2 FTOH) indicated that the displacement effect potentially occurred after 35 min of extraction when using the DVB/Car-WR/PDMS extraction phase. This is suggestive of a potential adsorption competition phenomenon between the polar fluoroalkyl alcohols and the more hydrophobic sulfonamides and sulfonamidoethanols. Collectively, our findings underscore the utility of tailoring SPME parameters to ensure optimal preconcentration and sensitivity for analysis of neutral volatile and semi-volatile PFAS. Future work would explore applying this methodology to a higher-resolution instrument, which may mitigate potential interferences in complex samples near the LOQ and enable the achievement of lower LOQs. In summary, this work highlights a promising new framework for expanding SPME applications for the extraction and preconcentration of volatile PFAS, as well as opens the door to understanding potential competitive adsorption effects which can occur in multicomponent systems.

Author contributions

Madison L. Williams: methodology, investigation, formal analysis, data curation, visualization, validation, writing – original draft; Stefan Cretnik: resources, methodology, writing – review & editing; Lucas Lüthy: resources, methodology, writing – review & editing; Tom Flug: resources, methodology, writing – review & editing; Michael Stebler: resources, methodology, writing – review & editing; Emanuela Gionfriddo: conceptualization, supervision, project administration, methodology, funding acquisition, resources, writing – review & editing.

Conflicts of interest

The authors declare no competing interests.

Data availability

The data supporting this article has been included as part of the SI and *via* Open Science (OSF) **https://osf.io/9xpuw/?view_only=8f0f20be7a6d44a28afaf69ec018d83d**.

Supplementary Information is provided, including: extraction time profiles, calibration curve equations with weighting, linear dynamic ranges, regression coefficients, analysis of variance, and representative chromatographic peaks at the limits of quantitation and detection for HS-SPME arrow and fiber devices. See DOI: **https://doi.org/10.1039/d5an00758e**.

Acknowledgements

The authors acknowledge funding from the Environmental Chemical Science and Chemical Measurement and Imaging Programs at the United States National Science Foundation (CHE-2432184).

References

1 M. Kotthoff, J. Müller, H. Jürling, M. Schlummer and D. Fiedler, *Environ. Sci. Pollut. Res.*, 2015, **22**, 14546–14559.
2 F. M. Hekster, R. W. Laane and P. de Voogt, *Rev. Environ. Contam. Toxicol.*, 2003, **179**, 99–121.
3 L. Jane, L. Espartero, M. Yamada, J. Ford, G. Owens, T. Prow and A. Juhasz, *Environ. Res.*, 2022, **212**, 113431.
4 E. M. Sunderland, X. C. Hu, C. Dassuncao, A. K. Tokranov, C. C. Wagner and J. G. Allen, *J. Exposure Sci. Environ. Epidemiol.*, 2019, **29**, 131–147.
5 T. Portolés, L. E. Rosales, J. V. Sancho, F. J. Santos and E. Moyano, *J. Chromatogr., A*, 2015, **1413**, 107–116.
6 J. M. Mattila, J. D. Krug, W. R. Roberson, R. P. Burnette, S. McDonald, L. Virtaranta, J. H. Offenberg and W. P. Linak, *Environ. Sci. Technol.*, 2024, **58**, 3942–3952.

7 J. Sun, W. Lorpaiboon, N. Fox, A. Jones, J. Ho, M. J. Manefield, N. Kumar, D. O'Carroll and M. Lee, *Water Res.*, 2025, **268**, 122717.
8 J. Hammer and S. Endo, *Environ. Sci. Technol.*, 2022, **56**, 15737–15745.
9 S. Endo, J. Hammer and S. Matsuzawa, *Environ. Sci. Technol.*, 2023, **57**, 8406–8413.
10 I. Abusallout, C. Holton, J. Wang and D. Hanigan, *J. Hazard. Mater. Lett.*, 2022, **3**, 100070.
11 Y. Wang and J. Pawliszyn, *Green Anal. Chem.*, 2023, **6**, 100070.
12 A. U. Rehman, M. Crimi and S. Andreescu, *Trends Environ. Anal. Chem.*, 2023, **37**, e00198.
13 C. Bach, V. Boiteux, J. Hemard, A. Colin, C. Rosin, J.-F. Munoz and X. Dauchy, *J. Chromatogr., A*, 2016, **1448**, 98–106.
14 J. Roth, I. Abusallout, T. Hill, C. Holton, U. Thapa and D. Hanigan, *Environ. Sci. Technol. Lett.*, 2020, **7**, 164–170.
15 H. Martínez-Pérez-Cejuela, M. L. Williams, C. McLeod and E. Gionfriddo, *Anal. Chim. Acta*, 2025, **1345**, 343746.
16 M. C. Corviseri, A. Polidoro, M. De Poli, C. Stevanin, T. Chenet, C. D'Anna, A. Cavazzini, L. Pasti and F. A. Franchina, *Talanta*, 2025, **292**, 127944.
17 R. Aranda-Rodriguez, A. Piperakis, J. Grandy, L. McGregor, N. Boegelsack, H. Calder, M. Edwards, W. Papas, J. Che and S. Shields, *J. Chromatogr., A*, 2024, **1733**, 465219.
18 I. K. Dimzon, J. Westerveld, C. Gremmel, T. Frömel, T. P. Knepper and P. de Voogt, *Anal. Bioanal. Chem.*, 2017, **409**, 1395–1404.
19 M. A. G. Wallace, M. G. Smeltz, J. M. Mattila, H. K. Liberatore, S. R. Jackson, E. P. Shields, X. Xhani, E. Y. Li and J. H. Johansson, *Chemosphere*, 2024, **358**, 142129.
20 M. N. Wieczorek, *Molecules*, 2024, **29**(21), 5137.
21 G. Ouyang and J. Pawliszyn, *TrAC, Trends Anal. Chem.*, 2006, **25**, 692–703.
22 J. Pawliszyn, in *Handbook of Solid Phase Microextraction*, ed. J. Pawliszyn, Elsevier, Oxford, 2012, pp. 61–97, DOI: **10.1016/B978-0-12-416017-0.00003-6**.
23 J. S. Herrington, G. A. Gómez-Ríos, C. Myers, G. Stidsen and D. S. Bell, *Separations*, 2020, **7**(1), 12.
24 M. Ziegler and H.-G. Schmarr, *Chromatographia*, 2019, **82**, 635–640.
25 J. Van Loco, M. Elskens, C. Croux and H. Beernaert, *Accredit. Qual. Assur.*, 2002, **7**, 281–285.
26 Z. Zhang and J. Pawliszyn, *Anal. Chem.*, 1993, **65**, 1843–1852.
27 J. Pawliszyn, D. Vuckovic, F. Mirnaghi and S. Risticevic, in *Handbook of Solid Phase Microextraction*, ed. J. Pawliszyn, Elsevier, Oxford, 2012, pp. 135–165, DOI: **10.1016/B978-0-12-416017-0.00005-X**.
28 C. Lancioni, C. Castells, R. Candal and M. Tascon, *Adv. Sample Prep.*, 2022, **3**, 100035.
29 J. Pawliszyn, in *Handbook of Solid Phase Microextraction*, ed. J. Pawliszyn, Elsevier, Oxford, 2012, pp. 13–59, DOI: **10.1016/B978-0-12-416017-0.00002-4**.
30 G. Ouyang, S. Cui, Z. Qin and J. Pawliszyn, *Anal. Chem.*, 2009, **81**, 5629–5636.
31 J. Xu, Q. Hu, X. Liu, S. Wei, J. Zheng, W. Lin, Y. Ye, F. Zhu and G. Ouyang, *J. Sep. Sci.*, 2020, **43**, 1847–1853.
32 A. Kremser, M. A. Jochmann and T. C. Schmidt, *Anal. Bioanal. Chem.*, 2016, **408**, 943–952.
33 M. Llambrich, N. Ramírez, R. Cumeras and J. Brezmes, *Anal. Chim. Acta*, 2024, **1329**, 343261.
34 E. Gionfriddo, É. A. Souza-Silva and J. Pawliszyn, *Anal. Chem.*, 2015, **87**, 8448–8456.